American Mineralogist, Volume 95, pages 456–462, 2010

Structural relaxation around Cr^{3+} and the red-green color change in the spinel (sensu stricto)-magnesiochromite ($MgAl_2O_4$-$MgCr_2O_4$) and gahnite-zincochromite ($ZnAl_2O_4$-$ZnCr_2O_4$) solid-solution series

Ulf Hålenius,[1,*] Giovanni B. Andreozzi,[2] and Henrik Skogby[1]

[1]Department of Mineralogy, Swedish Museum of Natural History, SE-10405 Stockholm, Sweden
[2]Dipartimento di Scienze della Terra, Sapienza Universitá di Roma, Piazzale Aldo Moro 5, I-00185 Roma, Italy

Abstract

Optical absorption spectra of flux-grown single crystals in the spinel s.s.-magnesiochromite and gahnite-zincochromite solid solutions were recorded with the aim of exploring variations in local Cr-O bond distance as a function of composition. With increasing Cr contents, the crystals vary in color from pale red to intensely red to dark greenish. These variations are reflected in the optical spectra by the position and intensity of the two spin-allowed electronic *d-d* transitions in six-coordinated Cr^{3+} at ~18 000 (ν_1) and 25 000 cm^{-1} (ν_2). From the shift of the ν_1 band position, a decrease in crystal field splitting, 10*Dq*, for six-coordinated Cr^{3+} with increasing Cr contents is evident in both solid-solution series. Based on published Cr-O bond distances for the CrO_6 polyhedra in magnesiochromite and zincochromite of 1.995 and 1.991 Å, respectively, and applying the ligand field relationships, local Cr-O bond distances in gahnite and spinel with Cr contents at trace levels are determined to be 1.974(2) and 1.960(3) Å, respectively. These local Cr-O distances result in relaxation parameters (ε) equal to 0.69(2) and 0.60(3) for Cr-O bonds in the $Mg(Al_{1-x}Cr_x)_2O_4$ and $Zn(Al_{1-x}Cr_x)_2O_4$ series, respectively. However, the presently obtained Racah *B* values indicate increasing Cr-O bond covalency with increasing Cr^{3+} contents. This suggests that color changes and accompanying 10*Dq* variations may be due to variations in Cr-O bond covalency along the two solid-solution series, without or with very minor local Cr-O bond distance variation. Consequently, the ε values obtained from the present optical absorption spectra should be regarded as minimum values.

Keywords: Crystal synthesis, optical spectroscopy, structural relaxation, spinel, gahnite, Cr^{3+}

Introduction

With increasing Cr content, color changes from pale red to dark green are often observed in solid solutions of different spinel end-members, as well as in other Cr-bearing oxygen-based mineral binary series (e.g., Poole 1964). These color changes are related to variations in optical absorption, and they are generally interpreted within the ligand field theory as expressions of variable Cr-O distances along the respective solid-solution series (e.g., Burns 1993). Since the ionic radius of six-coordinated Cr^{3+} (0.615 Å) is larger than that of Al^{3+} (0.535 Å), the accommodation of a size mismatch is expected to create either short-range or long-range structural modifications in the host structure.

Spectroscopic methods have demonstrated that the local structure often differs from the average structure as determined by diffraction methods, and that Vegard's rule is not obeyed at the atomic scale due to lattice relaxation during atomic substitution (Galoisy 1996). The relaxation coefficient ε [defined by Urusov (1992) on the basis of a geometrical model] would be 0.0 for no relaxation, i.e., the case of the "virtual crystal" model obeying Vegard's rule, and 1.0 for complete relaxation, i.e., the case of the "hard-sphere" model. Notably, for the hard sphere model, the ionic radii are constant and the whole structure is expected to take up all modifications upon chemical substitution. In contrast, the "virtual crystal" model assumes that the ions are located without local distortions at the "ideal" lattice sites of the average unit cell, and they are substituted without modification of the bond distances. A modified version of the virtual crystal model is the "local structure" model, in which the structure may distort locally, keeping the near-neighbor distances roughly constant. Based on optical spectroscopy and the point charge model, partial lattice relaxation has been suggested for several transition-metal-bearing solid-solution series of oxygen-based mineral structures as, e.g., garnet, corundum, andalusite, and olivine, with values of ε ranging from 0.5 to 0.8 (Langer 2001; Taran et al. 2004).

In contrast, almost constant local Cr-O bond distances, and hence ε values close to 1.0, have been suggested on the basis of results from EXAFS studies on spinel (Juhin et al. 2007), garnet (Juhin et al. 2008), and corundum structures (Gaudry et al. 2003, 2006). In the present work, we apply optical absorption spectroscopy to explore this suggested complete bond distance relaxation during the substitution of Al^{3+} by Cr^{3+} in spinel sensu stricto (s.s) and in gahnite ($ZnAl_2O_4$). Spinel s.s. and gahnite, as well as magnesiochromite ($MgCr_2O_4$) and zincochromite ($MgCr_2O_4$), are virtually normal spinels displaying limited or no intersite exchange, and consequently all Cr-Al substitutions may be regarded to take place at the six-coordinated cation site.

* E-mail: ulf.halenius@nrm.se

0003-004X/10/0004–456$05.00/DOI: 10.2138/am.2010.3388

EXPERIMENTAL METHODS

Crystal growth and thermal annealing

Single crystals along the two binary joins spinel s.s.-magnesiochromite and gahnite-zincochromite were synthesized by means of a flux-growth method. Analytical grade MgO, $Al(OH)_3$, Cr_2O_3, and ZnO were dehydrated and dried at elevated temperatures before mixing with $Na_2B_4O_7$, used as flux compound. Experimental charges of ~7 g were prepared by thorough grinding and mixing under acetone in an agate mortar. Successful flux/reactant ratios were found to be in the range 1.50–1.85 for spinel s.s.-magnesiochromite and 1.85–2.20 for gahnite-zincochromite. Strong fractionation of Cr into the spinel phase was noted in all experiments, and consequently the Cr concentration of the starting reactants was decreased relative to the intended nominal product concentration. The starting materials were transferred to 15 mL Pt/Au (5%) crucibles and were covered by a Pt lid. A muffle furnace was used for the thermal runs, which consisted of a rise in temperature to a plateau (normally 1200 or 1300 °C) that was maintained for 24 h to obtain complete dissolution and homogenization and, thereafter, a slow decrease in temperature (4 °C/h) to 900 °C. The zincochromite end-member was synthesized at 100 °C lower temperature to reduce Zn evaporation. For one run (MgCr 02), the slow cooling path was extended down to 600 °C, with the aim to promote a more ordered cation distribution. The slow cooling paths were terminated by shutting off the power to the heating elements and a more rapid cooling to room temperature. Successful runs consisted of octahedral spinel crystals, borate needles, and occasional eskolaite (α-Cr_2O_3) embedded in a borate-rich glass. The glass phase and borate crystals were dissolved in warm diluted HCl. The recovered spinel single crystal ranged in size up to ~1 mm, but typically they attained sizes in the range 200–300 µm. The largest and morphologically best developed crystals were obtained for compositions close to the end-members (Fig. 1).

Three crystals from the run MgCr 02 were subjected to thermal annealing experiments with the purpose of studying cation order/disorder effects. After acquisition of optical data, the crystals were embedded in Pt foil and disordered by annealing at 1000 °C for two hours and drop-quenching into water, with an estimated cooling time within 1 s. The annealing time should be sufficient to equilibrate the cation ordering, according to the results obtained on synthetic spinel s.s. by Andreozzi and Princivalle (2002). Finally, the same crystals were thermally treated from 1000 to 600 °C, following the cooling path (4 °C/h) of the synthesis procedure, to test if the original ordering state could be reproduced.

Optical absorption spectroscopy

Optical absorption spectra in the UV/VIS range (320–800 nm) were recorded at room temperature from double-sided polished single crystals. Absorber thickness was varied in response to the Cr contents and was in the range 20–260 µm as determined by means of a digital micrometer. Spectra were recorded during three cycles at a spectral resolution of 1 nm with a Zeiss MPM800 single beam microscope-spectrometer equipped with Zeiss Ultrafluar 10× condenser and objective lenses, a 75W Xenon arc light source and a photomultiplier detector. The accuracy of wavelength readings in the spectral range 18 000–25 000 cm^{-1} is better than 30 cm^{-1} as monitored by recording spectra of Ho_2O_3-doped and Pr_2O_3/Nd_2O_3-doped calibration standards (Hellma glass filters 666-F1 and 666-F7). The recorded spectra were fitted with Gaussian components using the Jandel Scientific software Peakfit 4.0. The UV-absorption edge was fitted by an exponential function.

Electron microprobe analysis

The chemical compositions of the studied single crystals were determined with a Cameca SX 50 electron microprobe operated at 20 kV and 15 nA, with an incident beam size of ~1 µm. No less than 5 spot analyses were collected from each area of optical measurements in the respective crystals. The ZAF-4/FLS software was utilized for data reduction and correction. Synthetic standards used were periclase (Mg), corundum (Al), sphalerite (Zn), and metallic Cr. Carefully characterized synthetic $MgAl_2O_4$ spinel single crystals (Andreozzi et al. 2000) served as reference samples.

RESULTS AND DISCUSSION

Crystal chemistry

Chemical compositions of 15 crystals selected along the $MgAl_2O_4$-$MgCr_2O_4$ solid-solution series range from 1 to 100% of the Cr end-member, and that of five crystals selected along the $ZnAl_2O_4$-$ZnCr_2O_4$ solid-solution series range from 2 to 100% of the Cr end-member (Table 1). The crystals used for optical absorption spectroscopy are in general quite homogenous as demonstrated by the uncertainties given in Table 1. In spite of this, a very limited number of crystals of intermediate solid solution composition show restricted heterogeneities, but variations in Cr contents are in those cases always <0.06 atoms per formula unit. Due to its tendency to form sp^3 covalent bonds, Zn is usually ordered at the four-coordinated T site and does not participate in the intersite exchange reaction with Al (O'Neill and Navrotsky 1983; O'Neill and Dollase 1994). Consequently, the cation distribution in our gahnite-zincochromite spinels can be considered as close to fully ordered and completely normal. Moreover, due to the strong preference of Cr for octahedral coordination, very low or no cation inversion is expected for

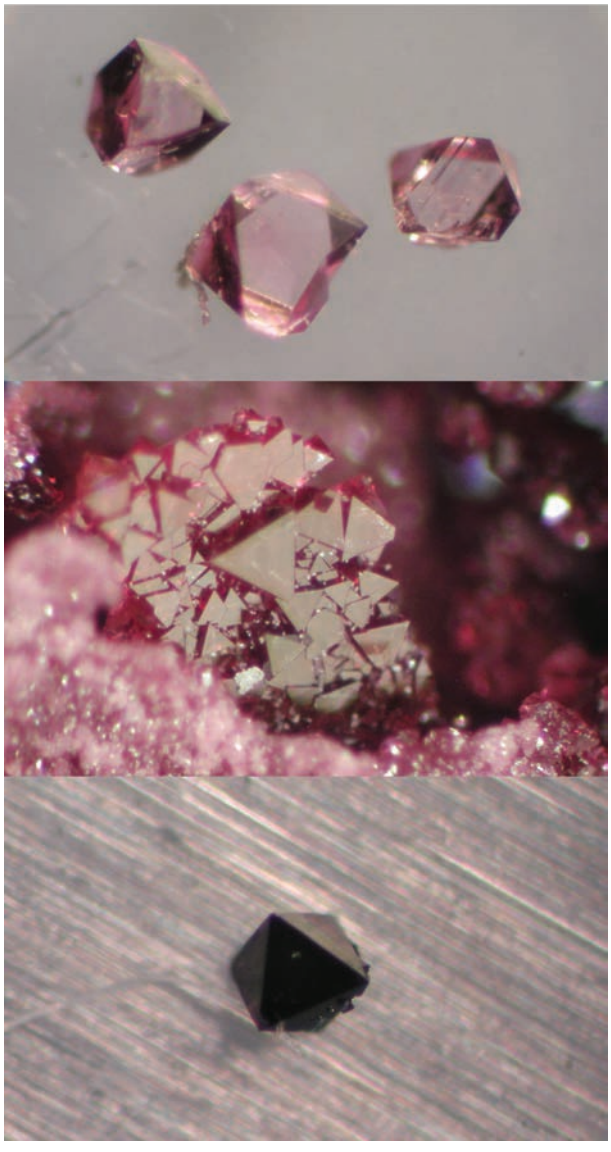

FIGURE 1. Microphoto of flux-grown $Mg(Al_{1-x}Cr_x)_2O_4$ crystals (x = 0.02, 0.45, 1.00 from top to bottom). The horizontal edge of the photos corresponds to 1 mm.

TABLE 1. Electron microprobe analyses of the present flux-grown $Mg(Al_{1-x}Cr_x)_2O_4$ and $Zn(Al_{1-x}Cr_x)_2O_4$ solid-solution crystals

Sample	MgCr 022	MgCr 023	MgCr 021	MgCr 05Br	MgCr 05Cr	MgCr 05Bc	MgCr 05Cc	MgCr05Cz	MgCr 3Aa	MgCr 5C	MgCr 7Aa
Al_2O_3 (wt%)	69.90(22)	69.05(26)	68.78(26)	68.25(95)	65.78(52)	64.76(62)	64.87(1.06)	59.38(28)	40.83(2.16)	38.27(60)	32.08(63)
Cr_2O_3	1.38(03)	2.14(07)	2.30(1.27)	3.91(1.22)	6.41(55)	7.19(59)	7.38(1.20)	13.36(65)	33.34(2.47)	36.29(69)	43.10(72)
MgO	28.37(23)	28.19(22)	27.96(11)	27.90(16)	27.71(16)	28.14(14)	27.94(15)	27.06(28)	25.24(21)	24.90(06)	24.18(16)
ZnO	nd	nd	nd	nd	nd	nd	nd	nd	nd	nd	nd
Sum	99.65	99.37	99.04	100.05	99.90	100.08	100.18	99.80	99.41	99.46	99.36
Cations on the basis of 4 O atoms per formula unit											
Al	1.967(26)	1.954(41)	1.953(21)	1.928(22)	1.877(11)	1.851(13)	1.852(21)	1.737(14)	1.288(58)	1.220(17)	1.051(17)
Cr	0.026(01)	0.041(01)	0.044(26)	0.074(23)	0.123(11)	0.138(12)	0.141(23)	0.262(13)	0.706(58)	0.777(16)	0.948(19)
Mg	1.01(05)	1.009(07)	1.004(05)	0.997(05)	1.000(07)	1.017(05)	1.009(03)	1.001(07)	1.008(01)	1.004(02)	1.002(04)
Zn	nd	nd	nd	nd	nd	nd	nd	nd	nd	nd	nd
Total	3.003	3.003	3.001	2.999	3.000	3.006	3.002	3.000	3.002	3.001	3.001
X $MgCr_2O_4/ZnCr_2O_4$	0.013(02)	0.021(01)	0.022(13)	0.037(12)	0.061(5)	0.069(6)	0.071(12)	0.131(07)	0.353(29)	0.388(8)	0.474(10)

Sample	MgCr 10	MgCr 15Ab	MgCr 20	MgCr 25	MgCr 50	MgCr 100B	ZnCr 1A	ZnCr 1B	ZnCr 5C	ZnCr 5D	ZnCr 100
Al_2O_3 (wt%)	24.65(1.05)	21.92(1.68)	11.66(15)	8.55(20)	2.01(08)	0.08(01)	53.62(34)	24.50(1.16)	19.30(07)	11.20(43)	0.09(05)
Cr_2O_3	51.30(1.09)	54.28(1.90)	65.63(40)	68.73(18)	76.53(20)	78.47(16)	1.64(07)	36.52(1.54)	43.42(43)	52.22(68)	66.32(33)
MgO	23.56(19)	23.04(16)	21.91(07)	21.60(02)	20.77(17)	20.69(13)	nd	nd	nd	nd	nd
ZnO	nd	nd	nd	nd	nd	nd	44.87(47)	39.19(43)	38.46(27)	36.26(16)	34.77(17)
Sum	99.52	99.24	99.20	98.88	99.31	99.24	100.13	100.21	101.18	99.68	101.22
Cations on the basis of 4 O atoms per formula unit											
Al	0.833(30)	0.752(53)	0.419(06)	0.313(07)	0.076(03)	0.003(00)	1.947(04)	0.999(44)	0.798(04)	0.487(17)	0.004(02)
Cr	1.163(31)	1.249(52)	1.583(08)	1.687(06)	1.932(06)	2.001(04)	0.040(02)	1.000(45)	1.204(09)	1.522(16)	2.006(04)
Mg	1.007(03)	0.999(04)	0.997(04)	1.000(02)	0.989(06)	0.994(06)	nd	nd	nd	nd	nd
Zn	nd	nd	nd	nd	nd	nd	1.020(06)	1.001(6)	0.996(09)	0.987(07)	0.982(05)
Total	3.003	3.000	2.999	3.000	2.997	2.998	3.007	3.000	2.999	2.996	2.995
X $MgCr_2O_4/ZnCr_2O_4$	0.581(16)	0.625(26)	0.792(04)	0.844(03)	0.966(02)	1.000(02)	0.020(01)	0.500(23)	0.602(05)	0.761(08)	0.998(02)

Notes: Values in parentheses represent standard deviations of five spot analyses. nd = not detected

Cr-rich compositions of both series. However, some disorder due to limited cation inversion should be taken into account for Cr-poor compositions of the $MgAl_2O_4$-$MgCr_2O_4$ solid-solution series, where temperature-dependent Mg-Al intersite exchange is expected. In fact, for stoichiometric $MgAl_2O_4$ crystals in equilibrium at 900 °C, a maximum cation inversion degree of 0.25 is expected (Andreozzi et al. 2000, 2001; Andreozzi and Princivalle 2002). A closure temperature of ~895 °C and a cation inversion degree decreasing from 0.25 to zero with increasing Cr content are estimated for all crystals of the present $MgAl_2O_4$-$MgCr_2O_4$ binary series, except MgCr 02 for which the closure temperature is estimated to be 780 °C and the inversion degree to be 0.23. Moreover, MgCr 02 crystals thermally annealed to 1000 °C are estimated to have an inversion degree of 0.27.

Optical spectra

The recorded optical absorption spectra (Figs. 2 and 3) of our spinel single crystals are in general agreement with published spectra of Cr-bearing spinels (e.g., Wood et al. 1968; Ikeda et al. 1997), showing two relatively weak and comparatively narrow absorption bands at ~29 000 and 15 000 cm^{-1} and two intense and broad absorption bands at ~24 000 (ν_2) and 18 000 (ν_1) cm^{-1}. The two former bands are caused by spin-forbidden transitions from the electronic ground state level $^4A_{2g}$ of the spectroscopic ^4F-state to the excited energy levels $^2A_{1g}$ and $^2T_{1g}$ of the ^2G-state. The position and intensity of the two latter absorption bands largely determine the crystal color, which varies from pale red via dark red to dark green with increasing Cr content. The two bands, ν_1 and ν_2, are related to the spin-allowed electronic *d-d* transitions between the spectroscopic states derived from the ^4F-state of the free ion, $^4A_{2g} \rightarrow {}^4T_{2g}(^4F)$ and $^4A_{2g} \rightarrow {}^4T_{1g}(^4F)$, respectively, in six-coordinated Cr^{3+}. These two transition energies directly define (Lever 1968) the crystal field splitting ($10Dq$) and the Racah interelectronic repulsion parameter (B) for $^{VI}Cr^{3+}$:

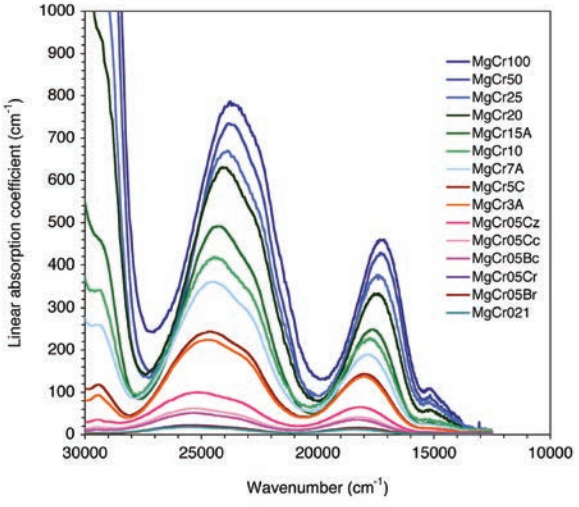

FIGURE 2. Room-temperature optical absorption spectra of the present $Mg(Al_{1-x}Cr_x)_2O_4$ crystals.

$10Dq = \nu_1$ and $B = (2\nu_1 - \nu_2)(\nu_2 - \nu_1)/(27\nu_1 - 15\nu_2)$.

Due to O atom displacements along [111], the point symmetry of the Cr^{3+}-bearing M site in spinel is lowered from O_h (ideal octahedron) to D_{3d} (trigonally distorted octahedron) (e.g., Andreozzi et al. 2000; Lenaz et al. 2006). As a consequence, each of the two excited spectroscopic ^4F-states in Cr^{3+} is split into two spin-allowed *d-d* transitions and hence four spin-allowed transitions between split ^4F-states in Cr^{3+} may be observed in spinel spectra. In this case, $10Dq$ and B parameters are calculated from the arithmetic mean of the energies of each of the two split transitions. The splitting of the band at ~24 000 cm^{-1} is evident in

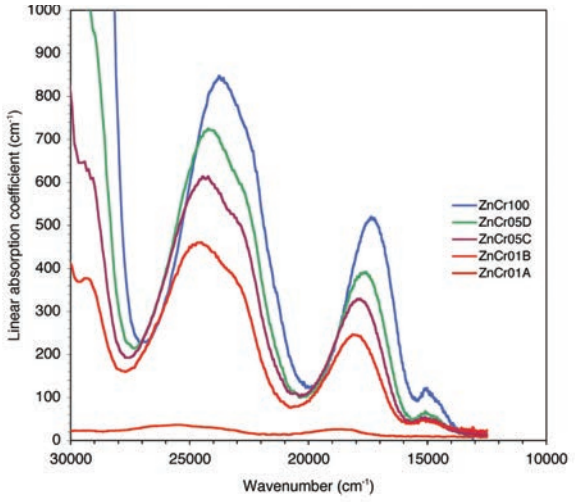

FIGURE 3. Room-temperature optical absorption spectra of the present $Zn(Al_{1-x}Cr_x)_2O_4$ crystals.

TABLE 2. Compositions, estimated closure temperatures, spin-allowed Cr^{3+} bands, Racah *B* value, and local Cr-O distances

Sample	ACr_2O_4 (fraction)	*T* (°C)	ν_1 (cm^{-1})	ν_2 (cm^{-1})	*B* (cm^{-1})	Local Cr-O (Å)
MgCr 022	0.013	780	18487	24794	604	1.973
MgCr 022		1000	18375	24706	608	1.976
MgCr 023	0.020	780	18464	24776	604	1.974
MgCr 023		1000	18346	24735	615	1.976
MgCr 021	0.022	780	18527	24793	599	1.972
MgCr 021		1000	18299	24706	617	1.977
MgCr 05Br	0.037	895	18420	24779	610	1.975
MgCr 05Cr	0.061	895	18382	24738	610	1.975
MgCr 05Bc	0.069	895	18407	24693	602	1.975
MgCr 05Cc	0.071	895	18360	24643	602	1.976
MgCr 05Cz	0.131	895	18313	24555	597	1.977
MgCr 3Aa	0.353	895	18163	24260	582	1.980
MgCr 5C	0.388	895	18157	24220	578	1.980
MgCr 7Aa	0.474	895	18011	24043	575	1.984
MgCr 10	0.581	895	17974	23947	568	1.984
MgCr 15Ab	0.625	895	17881	23847	568	1.986
MgCr 20	0.792	895	17698	23622	565	1.991
MgCr 25	0.844	895	17668	23528	558	1.991
MgCr 50	0.966	895	17570	23432	558	1.993
MgCr 100B	1.000	895	17518	23391	560	1.995
ZnCr 1A	0.020	895	18995	25114	579	1.961
ZnCr 1B	0.500	895	18272	24216	563	1.976
ZnCr 5C	0.602	895	18081	23973	558	1.980
ZnCr 5D	0.761	895	17900	23793	560	1.984
ZnCr 100	0.998	800	17576	23351	548	1.991

the present spectra by a distinct low-energy shoulder, while the splitting of the band at ~18 000 cm^{-1} is expressed by a distinctly skewed band shape, indicating that the split states derived from $^4T_{2g}$ (^4F) are closer in energy than the two states derived from $^4T_{1g}$ (^4F). In agreement with the present experimental observations and the theoretical study of $3d^3$-cations in trigonally distorted sites (Lever and Hollebone 1971), the two intense and relatively broad absorption bands recorded in our spectra were each fitted with two sub-bands representing the spin-allowed $^4A_{2g} \rightarrow {}^4E_g + {}^4A_{2g} \rightarrow {}^4A_{1g}$ and $^4A_{2g} \rightarrow {}^4E_g + {}^4A_{2g} \rightarrow {}^4A_{2g}$ *d-d* transitions in six-coordinated Cr^{3+} in a field of D_{3d} symmetry. The results of the spectrum fits are summarized in Table 2, which highlights the shift of the spin-allowed Cr^{3+} *d-d* bands toward lower energies with increasing Cr-contents in both of the present solid-solution series. In detail, the energy of the split $^4A_{2g} \rightarrow {}^4T_{1g}$ (ν_2) band decreases with ~1800 and 1400 cm^{-1} in the $Zn(Al_{1-x}Cr_x)_2O_4$ and $Mg(Al_{1-x}Cr_x)_2O_4$ series, respectively. The corresponding decrease in energy of the split $^4A_{2g}$-$^4T_{2g}$ (ν_1) band is ~1400 and 900 cm^{-1}, respectively (Fig. 4).

Local Cr-O distance

Within the framework of traditional ligand field theory, 10*Dq* values for individual transition metal cations (M) are directly related to the mean metal-oxygen (M-O) bond distance of the MO_n polyhedron. Based on the relation $10Dq = (CZ_Le^2/R^5)\langle r^4\rangle$, where *C* is a constant, Z_Le is the charge on ligands separated by the distance *R* from the central cation, and $\langle r^4\rangle$ is the mean value of the fourth power of the radial distribution of a 3*d* orbital from the nucleus, it should consequently be possible to extract relative local M-O distances from optical absorption spectra of cations in mineral structures. Provided that $(Z_Le^2)\langle r^4\rangle$ remains constant and that the M-O bond distance, $[(M\text{-}O)^{loc}]_{x=1}$, and the crystal field splitting parameter for the 3*d* metal cation, $(10Dq)_{x=1}$, in the 3*d* metal-rich end-member (x = 1) of a binary are known, it is possible to calculate the local M-O bond distance $[(M\text{-}O)^{loc}]_x$ for any given composition (x < 1) on a binary from the recorded crystal field splitting of that composition, $(10Dq)_x$, by applying the relation $[(M\text{-}O)^{loc}]_x = [(10Dq)_{x=1}/(10Dq)_x]^{1/5} \cdot [(M\text{-}O)^{loc}]_{x=1}$. However, several recent experimental and computational studies (e.g., García-Fernández et al. 2006; García-Lastra et al. 2008; Gaudry et al. 2006; Moreno et al. 2007) have demonstrated the limitations of this simple approach. These studies have clearly illustrated that the mean electrostatic potential (E_R) caused by all lattice atoms surrounding the actual metal-ligand complex may contribute substantially to the 10*Dq* of the central transition metal cation M. Consequently, comparative studies of local metal-ligand distances in different structures based exclusively on 10*Dq* values from optical absorption spectra and the point charge model may be misleading. The comparison between Cr^{3+} substituting for Al in beryl (emerald) and corundum (ruby) is particularly instructive in this context (Moreno et al. 2007).

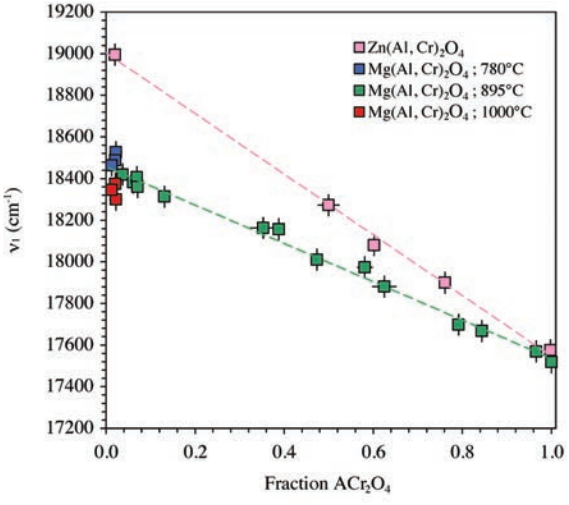

FIGURE 4. Plot of the energy of the spin-allowed ν_1-transition in six-coordinated Cr^{3+} (=10*Dq*) in the $Mg(Al_{1-x}Cr_x)_2O_4$ and $Zn(Al_{1-x}Cr_x)_2O_4$ solid solutions vs. spinel Cr concentration.

Although mean Al-O bond distances are comparable in these two minerals, 10*Dq* values for Cr^{3+} in corundum are experimentally determined to be ~2500 cm^{-1} higher than in beryl.

In the case of a transition metal cation in binary solid solutions with constant symmetry and in which the symmetry of the MO_n polyhedron remains unchanged in the entire composition range, the potential causes for variations in E_R are strongly restricted. This is the case for the present solid-solution series $Mg(Al_{1-x}Cr_x)_2O_4$ and $Zn(Al_{1-x}Cr_x)_2O_4$, for which no composition-dependent space group or point group changes occur at room temperature. The symmetry of the CrO_6 polyhedron is D_{3d} throughout the entire series, and consequently, variations in 10*Dq* values observed by optical absorption spectroscopy may be considered as reasonably reliable indications of local Cr-O bond distance variations. Based on a Cr-O bond distance for the CrO_6 polyhedron in magnesiochromite and zincochromite of 1.995 and 1.991 Å, respectively (O'Neill and Dollase 1994), and applying the ligand field relationships, local Cr-O bond distances in spinel s.s. and gahnite with Cr contents approaching zero, i.e., at trace levels, are determined to be 1.974(2) and 1.960(3) Å, respectively (Fig. 5; Table 2). Taking as reference the M-O distances of 1.928 and 1.914 Å determined for the spinel s.s and gahnite end-members, respectively (Andreozzi et al. 2000; O'Neill and Dollase 1994), ε values of 0.69 ± 0.02 and 0.60 ± 0.03 are determined from the optical spectra of our Mg- and Zn-bearing samples, respectively.

The recent EXAFS study on a natural spinel containing 1.03 wt% Cr_2O_3 (Juhin et al. 2007) reports a local Cr-O distance of 1.98 ± 0.01 Å, from which ε = 0.83 ± 0.14 was retrieved. From the crystal field splitting parameter of a sample with almost identical composition (MgCr 022, 1.38 wt% Cr_2O_3), we calculate, by applying the relation cited above, a local Cr-O bond distance of 1.973 ± 0.002 Å. It must be stressed that the uncertainty given for the latter distance refers exclusively to the uncertainty in the determination of the position of the ν_1 band in our optical spectra, under the assumption of the validity of the point charge model. Because the point charge model may not be fully valid and the uncertainty of the EXAFS-derived value is relatively large (see Fig. 5), there exists in fact no significant disagreement between the relaxation value based on EXAFS and the present ones based on optical absorption spectroscopy. Nonetheless, it should be noted that while the uncertainties in published EXAFS-based ε values make nearly complete relaxation around Cr^{3+} in Cr-doped spinel viable, our results point to a Cr-O bond relaxation slightly smaller than that suggested by EXAFS.

There are two potentially important reasons why optical absorption spectra may underestimate Cr-O bond relaxation in spinels. First, charge distribution variations in the second-nearest coordination sphere of the Cr^{3+} sites may vary due to different Mg-Al ordering at different Cr contents. Second, interactions between Cr atoms at neighboring M sites may cause composition dependent variations in Cr-O bond covalency. These two potential cases are briefly discussed in the following.

Earlier we stated that Cr may be regarded to substitute for Al exclusively at the six-coordinated M site and that Zn substitutes exclusively for Mg at the four-coordinated T site in the present spinel series (O'Neill and Navrotsky 1983; O'Neill and Dollase 1994). Consequently, the potential influence of variable degree

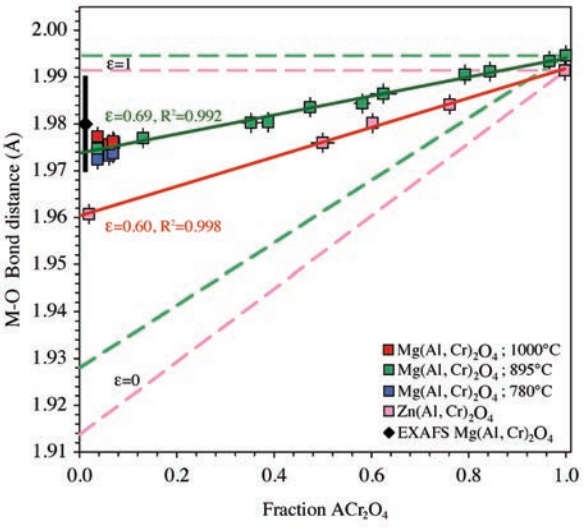

FIGURE 5. Local Cr-O bond lengths vs. Cr content in $Mg(Al_{1-x}Cr_x)_2O_4$ and $Zn(Al_{1-x}Cr_x)_2O_4$ solid solutions determined from the present optical absorption spectra on the basis of the point charge model. Experimental values for the Cr-O bond relaxation parameter, ε, are reported for both of the spinel solid-solution series. The broken lines represent Cr-O bond lengths for full (ε = 1) and no (ε = 0) Cr-O bond relaxation in the two series. Local Cr-O bond lengths determined by EXAFS in spinels samples with low Cr concentrations are reported for comparison (Juhin et al. 2007).

of cation ordering on the optical spectra of the $Zn(Al_{1-x}Cr_x)_2O_4$ series may be ruled out.

However, as previously mentioned, for spinels in the $Mg(Al_{1-x}Cr_x)_2O_4$ series, limited $^{IV}Mg^{2+}+{}^{VI}Al^{3+} \rightarrow {}^{IV}Al^{3+}+{}^{VI}Mg^{2+}$ intersite exchange can occur. This implies that the mean electrostatic potential, E_R, at CrO_6 polyhedra will vary with Cr content in this series. As the Mg-Al order-disorder reaction is temperature dependent, we have explored its effect on the 10*Dq* values by recording the optical spectra of three single crystals (samples MgCr 021, 022, and 023 in Table 2) of weakly Cr-doped spinels that were thermally treated to produce different cation distributions. Our spectra of these crystals show, in addition to marginal band broadening, distinct reversible shifts of the Cr^{3+} ν_1 band toward lower energies with increasing cation disorder (Fig. 6). The energy decrease (Table 2) in response to increasing cation disorder is significant but still comparatively small (~150 cm^{-1}). However, our experiments clearly demonstrate that a thermally induced increase in cation disorder results in decreasing 10*Dq* values, calculated local Cr-O distances, and relaxation parameters for Cr-bearing spinels (Figs. 4 and 5). As the results of the above experiments is opposite to the overall trend for the two present binary series, i.e., decreasing 10*Dq* values with decreasing cation disorder (at increasing Cr content), it is obvious that the effects of cation order-disorder reactions on the optical spectra and the determined 10*Dq* values cannot explain any potential underestimations of ε values in these spinels. A possible reason for the observed decrease in 10*Dq* values in response to increasing cation disorder in spinel s.s. is that the $^{IV}Mg^{2+}+{}^{VI}Al^{3+} \rightarrow {}^{IV}Al^{3+}+{}^{VI}Mg^{2+}$ intersite exchange reaction produces a significant change in the shape of the electrostatic potential acting upon the CrO_6 poly-

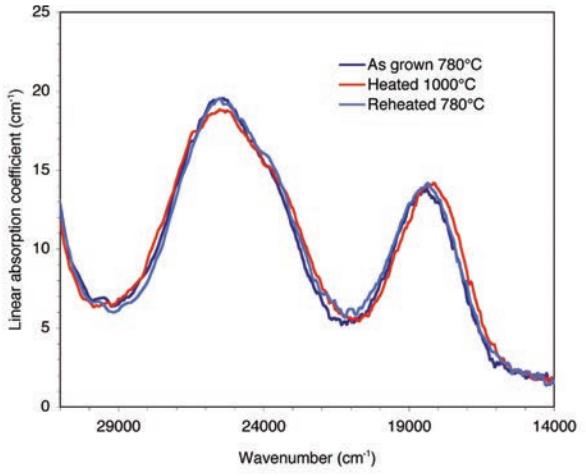

FIGURE 6. Room-temperature optical absorption spectra of a MgCr 02 spinel crystal subjected to thermal treatments resulting in different degrees of Mg-Al site exchange: inversion degree equals 0.23 at 780 °C and 0.27 at 1000 °C.

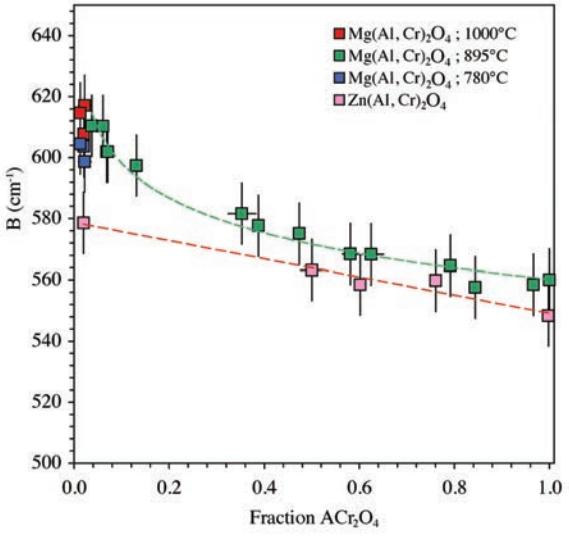

FIGURE 7. Variation in the Racah *B* parameter in response to Cr concentration in the $Mg(Al_{1-x}Cr_x)_2O_4$ and $Zn(Al_{1-x}Cr_x)_2O_4$ solid solutions.

hedra. Comparable effects have been observed in Cr^{3+}-bearing alkali fluorides with normal and inverse perovskite structures (Moreno et al. 2007).

Normally, bond covalency decreases (increasing *B* value) with increasing M-O bond distance (decreasing 10*Dq* value). This is nicely illustrated in, e.g., spectra of a Cr-bearing spinel (~8 mol% magnesiochromite) obtained at different temperatures (Taran et al. 1994), in which a thermally induced increase in local Cr-O bond distance resulting in a decrease in 10*Dq* value of ~550 cm^{-1} is accompanied by a *B* value increase of ~140 cm^{-1}. In both of the present spinel series, we observe decreasing *B* values with increasing Cr content (Fig. 7). This is unexpected, considering that our spectra show concomitantly decreasing 10*Dq* values.

Although it is qualitatively evident that an increasing number of Cr-centered six-coordinated M sites in the spinel series affects the internal electrostatic field, E_R, at the individual CrO_6 polyhedra, it is not a trivial task to quantify such effects, as demonstrated by recent ab-initio calculations of 10*Dq* for CrO_6 in corundum and beryl (García-Lastra et al. 2008), although some improvements in computational precision have been reported very recently (García-Lastra et al. 2009). Nevertheless, a crude estimate may be obtained from the interdependency of Cr-O bond covalency and 10*Dq* value observed by Taran et al. (1994). In the present spectra of the $Mg(Al_{1-x}Cr_x)_2O_4$ series, we observe at increasing Cr content a decrease in 10*Dq* of ~900 cm^{-1} that is accompanied by a decrease in *B* value of ~60 cm^{-1}. Provided that the 10*Dq* and *B*-value relationship observed in the thermal experiments of Taran et al. (1994) can be applied more generally to Cr-bearing spinels, it may be concluded that the 10*Dq* variations (and the red-green color change) observed in the two present solid-solution series may be entirely ascribed to covalency effects caused by variable Cr occupancies at next-nearest M sites. This implies that the local Cr-O bond length may be constant or very close to constant within the entire series and the resulting ε values calculated from optical absorption spectra should be regarded as minimum values.

ACKNOWLEDGMENTS

Financial support from the SYNTHESYS program (grant SE-TAF-3729; EC Research Infrastructure Action, FP6 Structuring the European Research Area) is gratefully acknowledged. The authors appreciate the microprobe analytical skills of H. Harryson (Uppsala University) and M. Serracino (CNR, IGAG-Rome). We appreciate useful comments by Bjorn Mysen, George Rossman, and an anonymous reviewer.

REFERENCES CITED

Andreozzi, G.B. and Princivalle, F. (2002) Kinetics of cation ordering in synthetic $MgAl_2O_4$ spinel. American Mineralogist, 87, 838–844.

Andreozzi, G.B., Princivalle, F., Skogby, H., and Della Giusta, A. (2000) Cation ordering and structural variations with temperature in $MgAl_2O_4$ spinel: An X-ray single crystal study. American Mineralogist, 85, 1164–1171.

Andreozzi, G.B., Lucchesi, S., Skogby, H., and Della Giusta, A. (2001) Compositional dependence of cation distribution in some synthetic $(Mg,Zn)(Al,Fe^{3+})_2O_4$ spinels. European Journal of Mineralogy, 13, 391–402.

Burns, R.G. (1993) Mineralogical Applications of Crystal Field Theory, 2nd edition, 551 p. Cambridge University Press, U.K.

Galoisy, L. (1996) Local vs. average structure round cations in minerals from spectroscopic and diffraction measurements. Physics and Chemistry of Minerals, 23, 217–225.

García-Fernández, P., García-Lastra, J.M., Aramburu, J.A., Barriuso, M.T., and Moreno, M. (2006) Strong dependence of 10 *Dq* on the metal-ligand distance: Key role played by the s-p hybrization on ligands. Chemical Physical Letters, 426, 91–95.

García-Lastra, J.M., Barriuso, M.T., Aramburu, J.A., and Moreno, M. (2008) Microscopic origin of the different colors displayed by $MgAl_2O_4:Cr^{3+}$ and emerald. Physical Review B, 78, 085117.

——— (2009) Color shift in $Al_2O_3{\cdot}xCr_2O_3$ solid solutions and the electroneutrality principle. Physical Review B, 79, 241106.

Gaudry, E., Kiratisin, A., Sainctavit, P., Brouder, C., Mauri, F., Ramos, A., Rogalev, A., and Goulon, J. (2003) Structural and electronic relaxations around substitutional Cr^{3+} and Fe^{3+} ions in corundum. Physical Review B, 67, 094108.

Gaudry, E., Sainctavit, P., Juillot, F., Bondioli, F., Ohresser, P., and Letard, I. (2006) From the green color of eskolaite to the red color of ruby: An X-ray absorption spectroscopy study. Physics and Chemistry of Minerals, 32, 710–720.

Ikeda, K., Nakamura, Y., Masumoto, K., and Shima, H. (1997) Optical spectra of synthetic spinels in the system $MgAl_2O_4$-$MgCr_2O_4$. Journal of the American Ceramic Society, 80, 2672–2676.

Juhin, A., Calas, G., Cabaret, D., Galoisy, L., and Hazemann, J.-L. (2007) Structural relaxation around substitutional Cr^{3+} in $MgAl_2O_4$. Physical Review B, 76, 054105.

——— (2008) Structural relaxation around substitutional Cr^{3+} in pyrope garnet. American Mineralogist, 93, 800–805.

Langer, K. (2001) A note on mean distances, $R_{(M'O6)}$, in substituted polyhedra

$[(M_{1-x}M'_x)O_6]$ in the crystal structures of oxygen based solid solutions: Local vs. crystal averaging methods. Zeitschrift für Kristallographie, 216, 87–91.

Lenaz, D., Skogby, H., Princivalle, F., and Hålenius, U. (2006) The $MgCr_2O_4$-$MgFe_2O_4$ solid solution series: Effects of octahedrally coordinated Fe^{3+} on T-O bond lengths. Physcis and Chemistry of Minerals, 33, 465–474.

Lever, A.B.P. (1968) Inorganic Electronic Spectroscopy, 420 p. Elsevier, Amsterdam.

Lever, A.B.P. and Hollebone, B.R. (1971) A theoretical study of the electronic spectra of trigonally distorted transition metal complexes. I. d^1, d^3, d^8 and d^9 complexes. Journal of the American Chemical Society, 94, 1816–1823.

Moreno, M., García-Lastra, J.M., Barriuso, M.T., and Aramburu, J.A. (2007) Transition metal impurities in wide gap materials: Are electronic properties well described through the ligand field theory? Theoretical Chemistry Accounts, 118, 665–671.

O'Neill, H.St.C. and Dollase, W.A. (1994) Crystal structures and cation distributions in simple spinels from powder XRD structure refinements: $MgCr_2O_4$, $ZnCr_2O_4$, Fe_3O_4, and the temperature dependence of cation distribution in $ZnAl_2O_4$. Physics and Chemistry of Minerals, 20, 541–555.

O'Neill, H.St.C. and Navrotsky, A. (1983) Simple spinels: Crystallographic parameters, cation radii, lattice energies, and cation distributions. American Mineralogist, 68, 181–194.

Poole Jr., C.P. (1964) The optical spectra and color of chromium containing solids. Journal of Physics and Chemistry of Solids, 25, 1169–1182.

Taran, M.N., Langer, K., Platonov, A.N., and Indutny, V.V. (1994) Optical absorption investigation of Cr^{3+} ion-bearing minerals in the temperature range 77–797 K. Physics and Chemistry of Minerals, 21, 360–372.

Taran, M.N., Langer, K., Abs-Wurmbach, I., Frost, D.J., and Platonov, A.N. (2004) Local relaxation around $^{[6]}Cr^{3+}$ in synthetic pyrope-knorringite garnets, $^{[8]}Mg_3{}^{[6]}(Al_{1-X}Cr_X^{3+})_2{}^{[4]}Si_3O_{12}$, from electronic absorption spectra. Physics and Chemistry of Minerals, 31, 650–657.

Urusov, V.S. (1992) A geometric model of deviations from Vegard's rule. Journal of Solid State Chemistry, 98, 223–236.

Wood, D.L., Imbusch, G.F., Macfarlane, R.M., Kisliuk, P., and Larkin, D.M. (1968) Optical spectrum of Cr^{3+} ions in spinels. Journal of Chemical Physics, 48, 5255–5263.

Manuscript received August 31, 2009
Manuscript accepted October 27, 2009
Manuscript handled by Bjorn Mysen